

In Silico Screening of the Phenolic Compound Oleuropein and Its Hydrolysis Product 3-Hydroxytyrosol Against Certain Structural and Non-Structural Proteins of SARS-CoV-2

Erman Salih İSTİFLİ^{1*}

¹Çukurova Üniversitesi, Fen-Edebiyat Fakültesi, Biyoloji Bölümü, Adana

*Sorumlu Yazar: esistifli@cu.edu.tr

Geliş Tarihi: 17.06.2021 Düzeltme Geliş Tarihi: 29.06.2021 Kabul Tarihi: 01.07.2021

Abstract

The novel corona virus has infected nearly 163 million people globally as of May 2021 and caused death of more than 3.3 million patients. Despite intense efforts, however, a small molecule with full therapeutic potential has not been developed in the treatment of SARS-CoV-2. The aim of this study was to investigate the inhibitory potentials of oleuropein and its hydrolysis product 3-hydroxytyrosol against spike glycoprotein, papain-like protease, main protease and RNA-dependent RNA polymerase of SARS-CoV-2 using molecular modelling simulations. Compared to 3-hydroxytyrosol, oleuropein showed stronger binding affinity to all targets in docking, and its affinity to Mpro ($-7.0 \text{ kcal mol}^{-1}$) and RdRp ($-8.0 \text{ kcal mol}^{-1}$) was quite high. Despite the Mpro-oleuropein complex, the RdRp-oleuropein complex showed a highly stable binding in 15-ns molecular dynamics based on root-mean-square-deviation (0.14 - 0.32 nm) and hydrogen bond numbers (6.85). The intracellular targets of oleuropein covered various proteases (17%), enzymes (16%), family A G protein-coupled receptors (11%), kinases (10%) and other cytosolic proteins (10%), however, probabilistic analysis showed that oleuropein was unlikely ($p = 0 - 0.22$) to bind these targets. ADMET profile showed that, with few exceptions, oleuropein has the physicochemistry that should be present in a drug molecule. In conclusion, oleuropein binds tightly to the active site of RdRp and could inhibit this enzyme. Oleuropein may be used alone or in combination with replicase inhibitors such as remdesivir or favipiravir in the treatment of COVID-19. Additional in vitro binding assays and in vivo efficacy studies are needed to prove our findings.

Key words: Oleuropein, 3-hydroxytyrosol, SARS-CoV-2, Molecular docking, Molecular dynamics

Fenolik Bileşik Oleuropein ve Hidroliz Ürünü 3-Hidroksitirozol'ün SARS-CoV-2'nin Bazı Yapısal ve Yapısal Olmayan Proteinlerine Karşı In Siliko Etkinliği

Öz

Yeni tip korona virüsü Mayıs 2021 itibarıyla dünya genelinde yaklaşık 163 milyon kişiyi enfekte etmiş ve 3.3 milyondan fazla hastanın ölümüne neden olmuştur. Yoğun çalışmalara rağmen SARS-CoV-2 tedavisinde tam koruma sağlayan terapötik potansiyelli bir ilaç geliştirilememiştir. Bu çalışmanın amacı, moleküler modelleme simülasyonları kullanarak oleuropein ve onun hidroliz ürünü 3-hidroksitirozol'ün SARS-CoV-2 spike glikoproteinini, papain-benzeri proteazı (PLpro), ana proteazı (Mpro) ve RNA-bağımlı RNA polimerazına (RdRp) karşı inhibitör potansiyellerini araştırmaktır. 3-hidroksitirozol ile karşılaştırıldığında oleuropein, moleküler doking analizinde tüm protein hedeflere daha yüksek bağlanma afinitesi göstermekle beraber Mpro ($-7.0 \text{ kcal mol}^{-1}$) ve RdRp'ye ($-8.0 \text{ kcal mol}^{-1}$) karşı afinitesi oldukça yüksek bulunmuştur. Kök-ortalama-kare-sapması (0.14 - 0.32 nm) ve hidrojen bağı sayısı (6.85) göz önüne alındığında, Mpro-oleuropein kompleksinin aksine, RdRp-oleuropein kompleksi 15 nanosaniyelik moleküler dinamik analizinde oldukça kararlı bir bağlanma sergilemiştir. Oleuropein'in intraselüler hedefleri arasında çeşitli proteazlar (%17), enzimler (%16), G protein-bağlı reseptörler (%11), kinazlar (%10) ve diğer sitozolik proteinler (%10) bulunmasına rağmen, olasılık analizlerine göre oleuropein'in bu hedeflere bağlanma olasılığı oldukça düşük bulunmuştur ($p = 0 - 0.22$). Birkaç istisna dışında oleuropein'in absorpsiyon-dağılım-metabolizma-atılım-toksitesite (ADMET) profili, bir ilaç molekülünde bulunması gereken fizikokimyasal özelliklere sahip olduğunu göstermiştir. Sonuç olarak oleuropein, RdRp'nin

aktif bölgesine sıkıca bağlanma ve bu enzimi inhibe etme potansiyeline sahiptir. Oleuropein, COVID-19 tedavisinde tek başına ya da remdesivir veya favipiravir gibi replikaz inhibitörleri ile birlikte kullanılabilir. Bulgularımızın kanıtlanması için ilave in vitro ilaç-bağlanma ve in vivo etkinlik çalışmalarına ihtiyaç duyulmaktadır.

Anahtar kelimeler: Oleuropein, 3-hidroksitirosol, SARS-CoV-2, Moleküler doking, Moleküler dinamik

Introduction

Severe acute respiratory syndrome coronavirus-2 (SARS-CoV-2), a highly contagious virus, causes coronavirus disease (COVID-19) that affects the respiratory system. Since the disease first appeared in Wuhan, China in December 2019, the disease was named COVID-19 (Raoult et al., 2020). Having crown-like spikes on its surface, the corona virus is classified into four subgroups known as alpha, beta, gamma and delta (Fehr and Perlman, 2015). The RNA genome of SARS-CoV-2, consisting of 29.891 base pairs, is 79.6% similar to SARS-CoV (Denison et al., 2011).

Just as SARS-CoV, SARS-CoV-2 also utilizes angiotensin converting enzyme 2 (ACE2) receptor on the surface of the host cells to initiate infection (Hoffmann et al., 2020). Therefore, the details of the molecular interactions between the spike glycoprotein (S) of the virus and the host ACE2 receptors are still an active area of research (Monteil et al., 2020). In addition, many research groups and leading pharmaceutical companies around the world have made extraordinary efforts to develop an effective vaccine against SARS-CoV-2 (Jackson et al., 2020). Today, thanks to various types of vaccines developed by countries such as England, America, Germany, China and Russia, a more effective fight against COVID-19 has started.

It has been known for a long time that all parts of the olive plant, *Olea europaea*, contain phenolic compounds such as oleuropein, 3-hydroxytyrosol, demethyl-oleuropein, ligstroside, and oleoside, which have various pharmacological effects, and quantitatively, oleuropein and 3-hydroxytyrosol are the most abundant phenolic compounds among these components (Omar, 2010). Anti-viral properties of oleuropein against herpes mononucleosis, hepatitis virus, rotavirus, bovine rhinovirus, canine parvovirus, feline leukemia virus, respiratory syncytial virus and para-influenza type 3 virus have been demonstrated in various studies (Ma et al., 2001). In addition, it has been suggested that the oleuropein contained in olive leaf extract has an inhibitory affinity on HIV-1 gp41 protein (surface glycoprotein subunit), which the HIV virus recruits in its entry into normal cells (Lee-Huang et al., 2007). These studies provide

clear evidence that oleuropein may undergo inhibitory molecular interactions with viral proteins.

The aim of this study was therefore to investigate the potential of oleuropein and 3-hydroxytyrosol to inhibit certain structural and non-structural proteins of SARS-CoV-2 by *in silico* methods and to determine a new hit compound in the treatment of SARS-CoV-2. For this purpose, the inhibitory potential of oleuropein and 3-hydroxytyrosol on SARS-CoV-2 certain structural (spike) and non-structural (PLpro, Mpro and RdRp) proteins was investigated using molecular docking and molecular dynamics techniques.

Materials and methods

Protein and ligand preparation

The resolved crystal structures of spike glycoprotein receptor binding domain (PDB ID: 6M17), Mpro (PDB ID: 6LU7), PLpro (PDB ID: 7NFV) and RNA-dependent RNA polymerase (RdRp) (PDB ID: 7D4F) were retrieved from Protein Data Bank with resolutions of 2.90 Å, 2.16 Å, 1.42 Å and 2.57 Å, respectively. Protonation states of ionisable side chains were assigned using the PropKa module of Vega ZZ (Li et al., 2005). The geometry of all proteins were minimized *via* the NAMD (nanoscale molecular dynamics) module of Vega ZZ software using a number of time steps of 15.000 (Pedretti et al., 2004). The 3D conformer of oleuropein (Figure 1) tested in this study was drawn in ChemOffice version 19.1 and then saved in pdb format. The Automatic Topology Builder (ATB) online server was utilized for the energy minimization of oleuropein ligand using the semi-empirical quantum mechanical (QM) self-consistent field (SCF) method (Malde et al., 2011). After geometry optimization, the minimized 3D ligand structure generated by the ATB server was exported in pdb file format for further use in molecular docking and dynamic simulations.

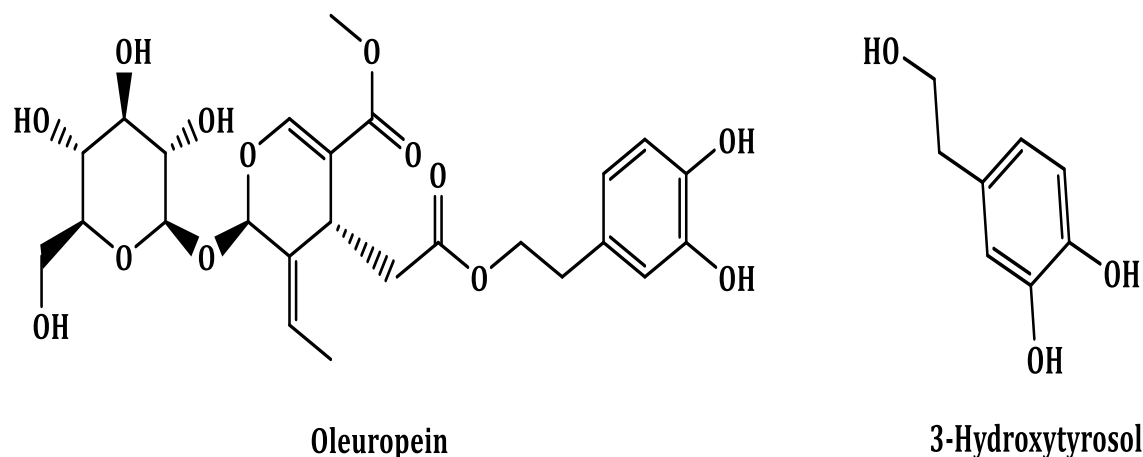


Figure 1. Chemical structures of oleuropein and 3-hydroxytyrosol

Molecular docking

In this study, molecular docking analysis was performed with two different programs (AutoDock 4.2.6 and AutoDock Vina) to find the most favorable binding energies of oleuropein and 3-hydroxytyrosol against 4 different enzymes. Therefore, protein-ligand complexes (Table 1) obtained with AutoDock Vina (cut off value = -7.0 kcal mol⁻¹) were subjected to molecular dynamic analysis. In this context, AMDock

(<https://github.com/Valdes-Tresanco-MS/AMDock-win>) assisted molecular docking tool with AutoDock Vina was implemented (Trott and Olson, 2010; Valdes-Tresanco et al., 2020). The grid box coordinates were set to allow the oleuropein ligand to interact with the catalytic amino acid residues of these target proteins (Wang et al., 2020).

Table 1. Comparison of oleuropein and 3-hydroxytyrosol docking scores (binding free energy) against SARS-CoV-2 certain structural and non-structural proteins calculated by AutoDock 4.2.6 and AutoDock Vina

Protein	Ligand	AutoDock 4.2.6	AutoDock Vina
		BFE	BFE
Spike (S)	Oleuropein	-5.36	-6.2
Spike	3-Hydroxytyrosol	-4.67	-5.0
Mpro (Nsp5)	Oleuropein	-6.97	-7.0
Mpro	3-Hydroxytyrosol	-4.65	-4.5
RdRp (Nsp12)	Oleuropein	-4.31	-8.0
RdRp	3-Hydroxytyrosol	-4.10	-5.3
PLpro (Nsp1)	Oleuropein	-5.07	-5.1
PLpro	3-Hydroxytyrosol	-4.91	-4.2

BFE: Binding free energy (ΔG° , kcal mol⁻¹)

Molecular dynamic simulation of Mpro-oleuropein and RdRp-oleuropein complexes

To analyze the stability of binding of Mpro-oleuropein and RdRp-oleuropein complexes, MD simulations were performed using the GROMACS 2020.1 version based on the docked

conformation of oleuropein with the Mpro and RdRp (Abraham et al., 2015). Details of the molecular dynamic simulations can be found elsewhere (Berendsen et al., 1981).

Target prediction and ADMET profile

In this study, web-based SwissTargetPrediction (<http://www.swisstargetprediction.ch/>) and pkCSM small-molecule pharmacokinetics (<http://biosig.unimelb.edu.au/pkcsm/>) servers were used to determine the biological safety profile of oleuropein (Daina et al., 2019; Pires et al., 2015).

Statistical analysis

Data were analyzed with one-way ANOVA using Tukey's test ($p < 0.05$).

Results and Discussion

The top-ranked conformation of oleuropein in the active site of Mpro is shown in Figure 2A. Molecular docking analysis showed that oleuropein firmly fits the active site of the enzyme surrounded by His41, Phe140, Asn142, His164, Met165, Gln192 and Arg403. The contacts of oleuropein with these residues consist of five H-bonds, two carbon-hydrogen bonds and one pi-sulfur interaction.

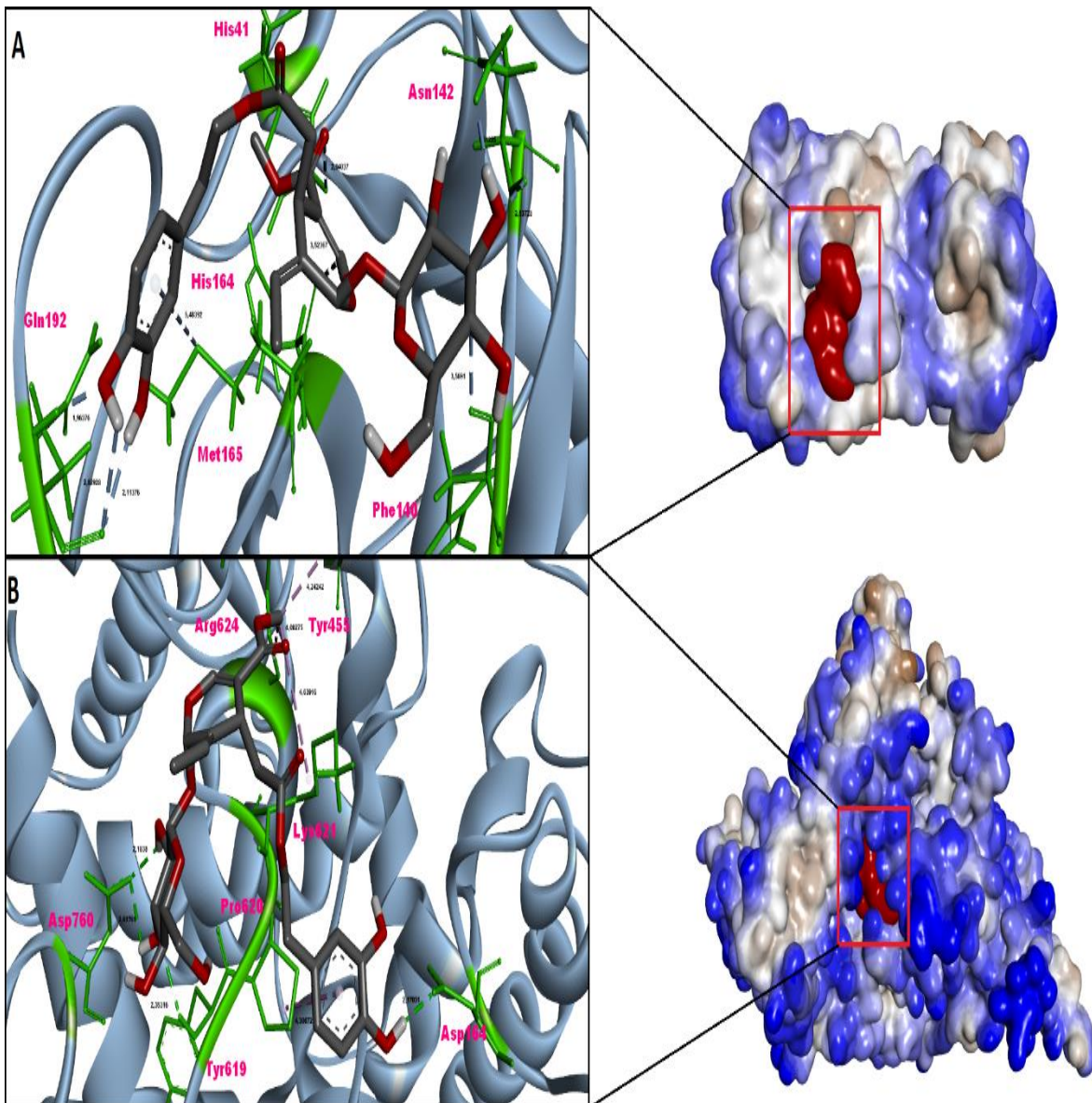


Figure 2. Top ranked conformations of oleuropein. (A- Mpro-oleuropein complex, B- RdRp-oleuropein complex). The 3D view on the right is shown in hydrophobicity surface mode and the regions circled by the red boxes show the binding conformation of oleuropein into the binding cavities of both enzymes

In addition, a large number of Van der Waals interactions stand out in the interaction of oleuropein with Mpro (Table 2). The top-ranked conformation of oleuropein with RdRp is shown in Figure 2B. Visual analysis of this complex showed that oleuropein snug fit into the active site (palm domain) surrounded by Asp164, Tyr455, Tyr619, Pro620, Lys621, Arg624 and Asp760. These interactions mainly consist of a total of four H-bonds, two pi-alkyl bonds and two alkyl bonds. Apart from these polar and non-polar interactions, a large number of Van der Waals interactions also stabilize the interaction of oleuropein with the active site of RdRp (Table 2). Therefore, in the interactions of oleuropein with the RdRp, it can be clearly concluded that H-bonding, non-polar and Van der Waals interactions play major role in the receptor-ligand complexation. In a phytochemical-based molecular docking study performed by Khaerunnisa et al. (2020), oleuropein was bound to the SARS-CoV-2 Mpro active site with a binding free energy of -7.31 kcal mol⁻¹. Consistent with our study, Khaerunnisa et al. reported that oleuropein formed H-bonds with the aminoacids Tyr54, Leu141, His163, and Glu166 of Mpro. In addition, oleuropein interacted highly favorably with Nsp15, a SARS-CoV-2 endoribonuclease, and formed electrostatic contacts with 11 residues, Van der Waals contacts with 5 residues, and a total of 4 H-bonds with 3 residues of this enzyme. It has been further reported that the functional groups that contribute most to the formation of the H-bonds in this interaction were the -OH and 3-methylene-4H-

pyran moieties of the oleuropein molecule (Vijayan and Gourinath, 2021). In a drug repurposing study performed with the Glide docking module, oleuropein exhibited -9.21 kcal mol⁻¹ (in the absence of Mg²⁺) and -6.07 kcal mol⁻¹ (in the presence of Mg²⁺) docking scores against the RdRp enzyme (Kandeel et al., 2020). However, in another molecular docking study performed with Chimera 1.8.1, oleuropein showed a binding affinity of -4.59 kcal mol⁻¹ to RdRp and interacted with the amino acids Asp445, Asp452, Tyr455 and Asn552 (Abd El-Aziz et al., 2020). This reported binding free energy value is considerably lower (rather weak) compared with the highly favorable binding affinity (-8.0 kcal mol⁻¹) in our study. Thus, it could be also proposed that the amino acid composition of the targeted region on the enzyme also plays a major role in the strength of the binding energy. Root-mean-square-deviation (RMSD) analysis of oleuropein-Mpro complex during the simulation showed that the RMSD did not reach an equilibrium and fluctuated between 0.09 nm and 0.37 nm (Figure 3). During the 15-ns simulation, the average number of hydrogen bonds formed between the oleuropein molecule and the receptor was 1.1 (Figure 4). Compared to Mpro-oleuropein complex, the RMSD of oleuropein in the RdRp-oleuropein complex was generally more stable and showed some variation between 0.14 nm and 0.32 nm (Figure 5). The number of hydrogen bonds formed between oleuropein and RdRp during the 15-ns simulation was highly stable and it was 6.85 on average (Figure 6).

Table 2. Molecular interactions of oleuropein with non-structural proteins of SARS-CoV-2, the main protease (Mpro) and RNA-dependent RNA polymerase (RdRp)

N	Enzym	Compou	Binding energy (kcal m)	Calculat inhibitic constan (μM)	Classic H-bond	Van der Waals	Non-Classi H-bond (C-H, π-Doi	Hydrophobic interac		Electrost.	Miscellane (π-sulfur)
								π-π interact	Mixed π/Alkyl		
1	Mpro	Oleurop	-7.00	7.40	His41 ^a , Asn142, Gln192	Met49, Leu1 Cys145 ^a , His Glu166 ^a , Leu Pro168 ^a , Arg Gln189 ^a , Thr ^a , Ala191 ^a Val166, Glu1 Lys551, Arg5	His164, Phe140	-	-	-	Met165
2	RdRp	Oleurop	-8.00	1.37	Asp164, Asp760, Tyr619	Asp618, Cys623, Phe Met794, Ser798	-	-	Tyr455, Pro Lys621, Arg	-	-

^a The active amino acid residues of SARS-CoV-2 Mpro (His41, Ser46, Leu141, Asn142, Cys145, Glu166, Pro168, Gln189, Thr190, Ala191)

^b The active amino acid residues of SARS-CoV-2 RdRp (Gly590, Ser592, Tyr595, Thr687, Tyr689, Leu758, Ser759, Asp760, Asp761, Cys813, Ser814)

Protein RMSD vs Lig RMSD

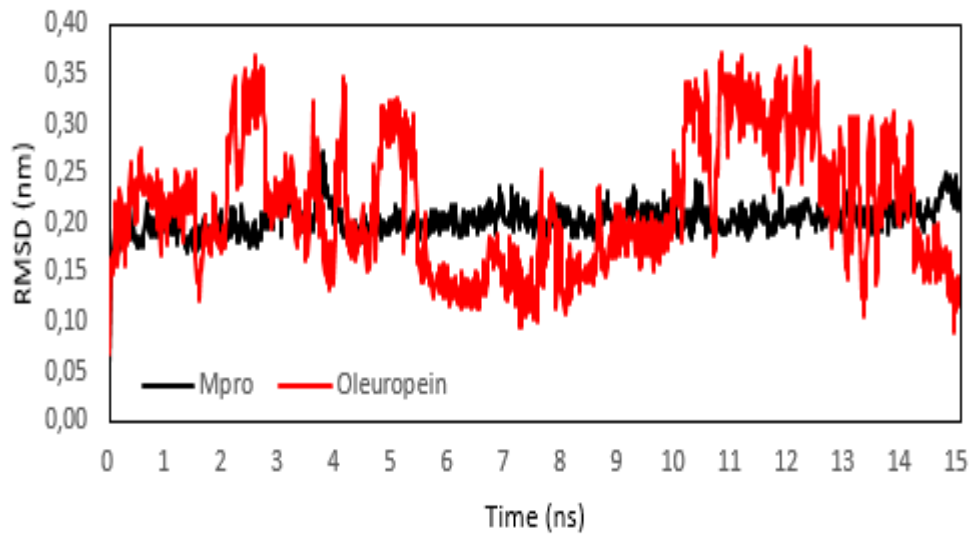


Figure 3. RMSD plots of SARS-CoV-2 main protease (Mpro) and oleuropein

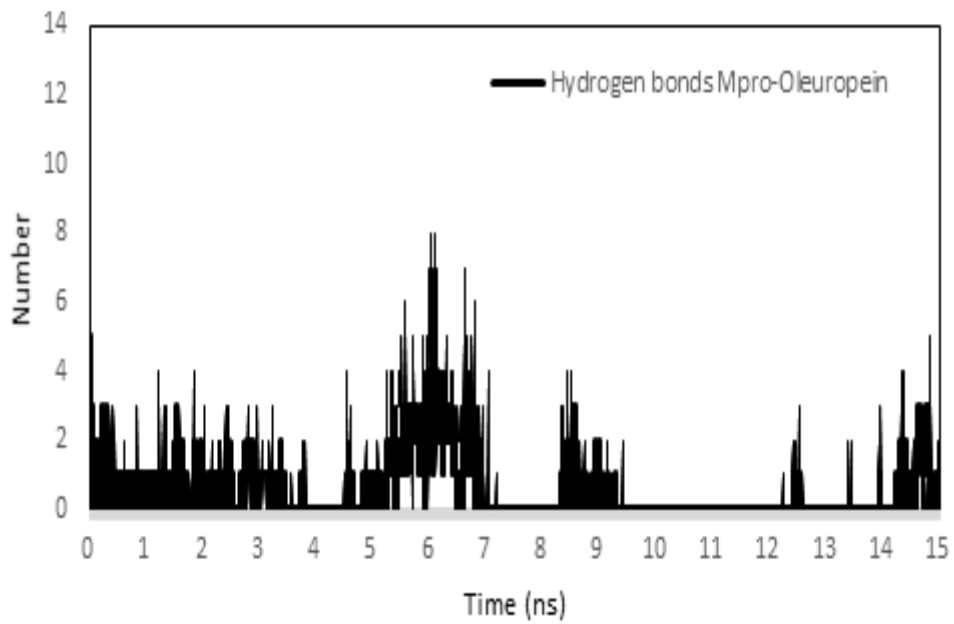


Figure 4. The number of hydrogen bonds between SARS-CoV-2 main protease (Mpro) and oleuropein

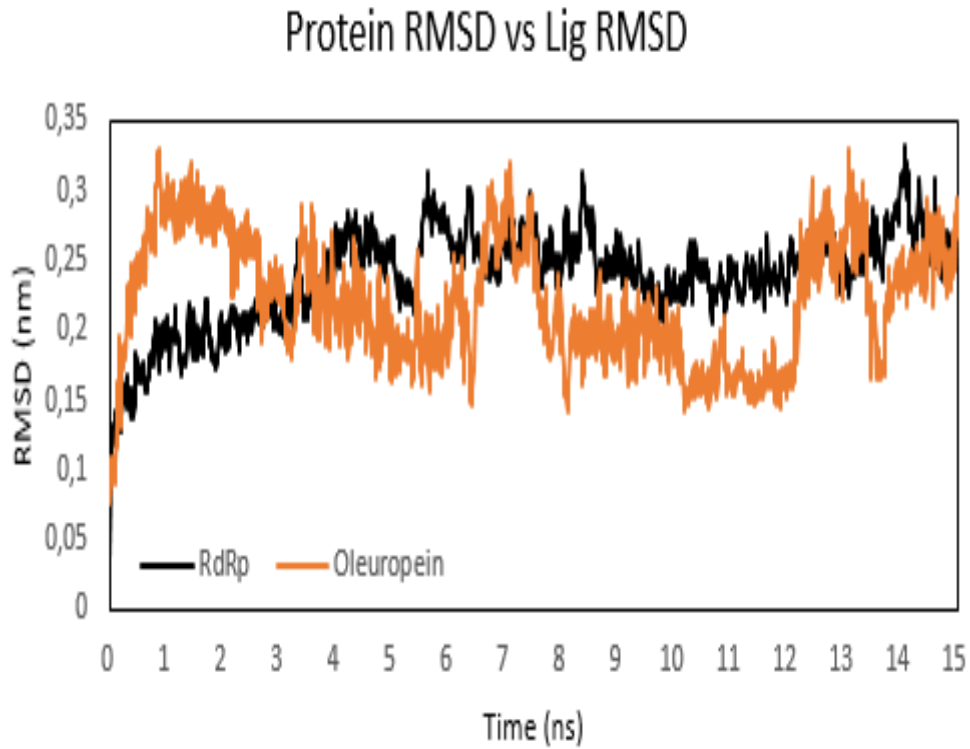


Figure 5. RMSD plots of SARS-CoV-2 RNA-dependent RNA polymerase (RdRp) and oleuropein

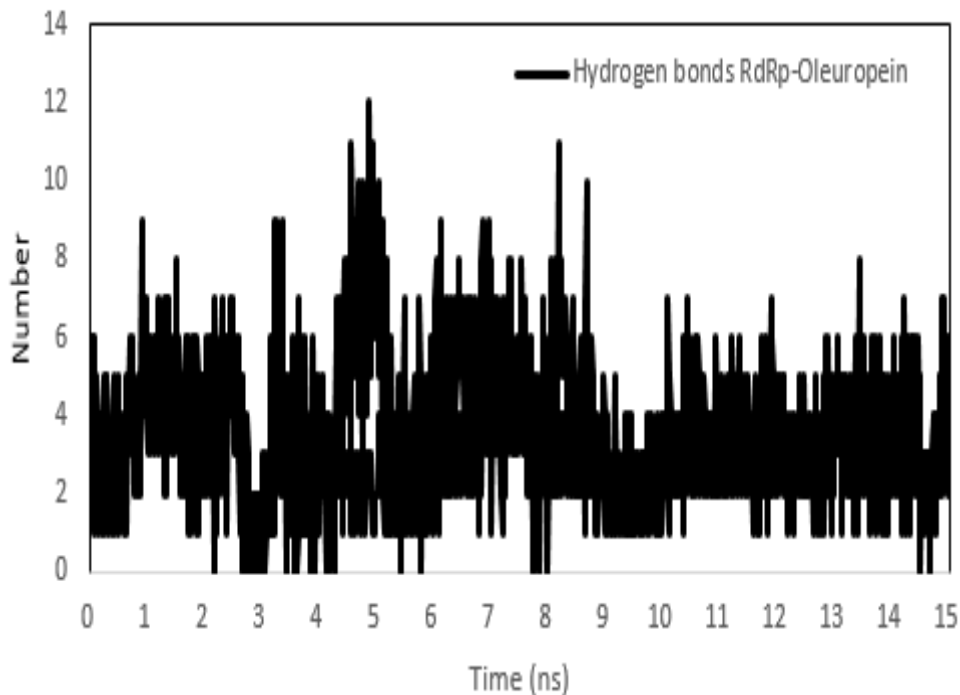


Figure 6. The number of hydrogen bonds between SARS-CoV-2 RNA-dependent RNA polymerase (RdRp) and oleuropein

In this study, the interaction of oleuropein with Mpro did not show stability in molecular dynamics simulation. On the other hand, the interactions of oleuropein with the active site of RdRp remained stable and strong throughout the

entire simulation (Figures 5 and 6). It has been suggested that effective SARS-CoV-2 RdRp inhibitors should have the ability to block translocation or impair RNA polymerization (Vicenti et al., 2021). Oleuropein, which was

subjected to docking and molecular dynamics simulations in our study, contains a large number of -OH groups bound to its glucose and 3-hydroxytyrosol subunits (Figure 1). Therefore, the stability resulting from the high number of H-bonds formed between the H atom in the -OH groups of oleuropein and the electron pairs on the heteroatoms (such as N, O) of RdRp strengthens the receptor-ligand interaction. Similarly, hydrogen bonds formed between electron pairs on C = O (carbonyl) or oxygen (-O-) atoms in oleuropein and H atoms bonded to heteroatoms (such as N, O) of RdRp also contribute to the stability of the receptor-ligand interaction (Sarikurkcu et al., 2021). Via this mechanism, oleuropein bound to the palm domain of RdRp may effectively inhibit viral replication by blocking translocation reaction or by preventing viral RNA from entering the replication site.

According to SwissTargetPrediction server, the putative intracellular targets of oleuropein have been found as various proteases (17%), enzymes (16%), family A G protein-coupled receptors (11%), kinases (10%) and other cytosolic proteins (10%), respectively. However, probability analyzes based on this server also show that the interaction values of oleuropein with these proteins are between 0.0 and 0.22 (http://www.swisstargetprediction.ch/result.php?job=1755753892&organism=Homo_sapiens). Thus, oleuropein is unlikely to bind to any off-target protein in the cell. Similarly, considering the ADMET profile of oleuropein based on the pkCSM server, it appears that this compound generally meets the ADMET criteria that should be present in a candidate drug molecule. However, oleuropein also causes hERGII inhibition, is a substrate of P-glycoprotein and induces toxicity in *T. pyriformis* (<http://biosig.unimelb.edu.au/pkcsml/>).

Conclusions

The current SARS-CoV-2 pandemic has made it crucial to discover new vaccine and drug molecules globally due to the frequent escape mutations of the virus and the emergence of new host receptors it uses to enter the cell. In addition to this drawback, considering that the success rate of producing a new vaccine or novel synthetic drug from the scratch is 15% and 10% respectively (Altay et al., 2020), *in silico* screening of organic phytochemicals against the SARS-CoV-2 infectious proteins can remarkably accelerate new drug discovery process. As a result of this *in silico* study, we found that oleuropein is a potential inhibitor of SARS-CoV-2 RNA-dependent RNA polymerase rather than the main protease. Oleuropein has the potential to inhibit the cellular replication process of the SARS-CoV-2 virus by binding with high affinity to

amino acid residues in the palm domain, which is defined as the active site of RdRp, and the number of formed H-bonds throughout the entire simulation reveals the strength of this binding. Furthermore, this organic compound neither show high binding affinity for intracellular enzymes and proteins nor violate ADMET rules significantly. Considering the fact that phytochemicals are natural inhibitors of viral proteins (Chojnacka et al., 2020), the use of oleuropein alone or in combination with replicase inhibitors remdesivir or favipiravir may lead to a good treatment strategy in patients with COVID-19 infection. Finally, if our findings are supported by *in vitro* drug binding assays and *in vivo* efficacy studies, oleuropein's ability to be a potential therapeutic COVID-19 antiviral agent can then be proved.

Conflict of Interest Statement: The author of the manuscript declares that there is no conflict of interest.

Contribution Rate Statement Summary: The writing of the article was performed by the author.

Acknowledgment: The author would like to thank to Dr. Selçuk AKTÜRK for his significant contribution at literature searching stage regarding the phytochemical content of the olive plant.

References

- Abd El-Aziz, N.M., Shehata, M.G., Awad, O.M.E., El-Sohaimy, S.A. 2020. Inhibition of COVID-19 RNA-Dependent RNA Polymerase by Natural Bioactive Compounds: Molecular Docking Analysis. Preprints (In press). DOI: <https://doi.org/10.21203/rs.3.rs-25850/v1>.
- Abraham, M.J., Murtola, T., Schulz, R., Páll, S., Smith, J.C., Hess, B., Lindahl, E. 2015. GROMACS: High performance molecular simulations through multi-level parallelism from laptops to supercomputers. *SoftwareX*, 1–2, 19-25.
- Altay, O., Mohammadi, E., Lam, S., Turkez, H., Boren, J., Nielsen, J., Uhlen, M., Mardinoglu, A. 2020. Current Status of COVID-19 Therapies and Drug Repositioning Applications. *iScience*, 23, 101303.
- Berendsen, H.J., Postma, J.P., van Gunsteren, W.F., Hermans, J. 1981. Interaction models for water in relation to protein hydration, in: B., P. (Ed.), *Intermolecular forces*, 331-342.
- Chojnacka, K., Witek-Krowiak, A., Skrzypczak, D., Mikula, K., Młynarz, P. 2020. Phytochemicals containing biologically

- active polyphenols as an effective agent against Covid-19-inducing coronavirus. *J. Funct. Foods*, 73, 104146.
- Daina, A., Michielin, O., Zoete, V. 2019. SwissTargetPrediction: updated data and new features for efficient prediction of protein targets of small molecules. *Nucleic Acids Res*, 47, 357-364.
- Denison, M.R., Graham, R.L., Donaldson, E.F., Eckerle, L.D., Baric, R.S. 2011. Coronaviruses: an RNA proofreading machine regulates replication fidelity and diversity. *RNA Biol*, 8, 270-279.
- Fehr, A.R., Perlman, S. 2015. Coronaviruses: an overview of their replication and pathogenesis. *Coronaviruses*, 1282, 1-23.
- Hoffmann, M., Kleine-Weber, H., Schroeder, S., Krüger, N., Herrler, T., Erichsen, S., Schiergens, T.S., Herrler, G., Wu, N.-H., Nitsche, A. 2020. SARS-CoV-2 cell entry depends on ACE2 and TMPRSS2 and is blocked by a clinically proven protease inhibitor. *Cell*, 181, 271-280.
- Jackson, L.A., Anderson, E.J., Roupael, N.G., Roberts, P.C., Makhene, M., Coler, R.N., McCullough, M.P., Chappell, J.D., Denison, M.R., Stevens, L.J. 2020. An mRNA vaccine against SARS-CoV-2—preliminary report. *New Engl. J. Med.*, 383, 1920-1931.
- Kandeel, M., Kitade, Y., Almubarak, A. 2020. Repurposing FDA-approved phytomedicines, natural products, antivirals and cell protectives against SARS-CoV-2 (COVID-19) RNA-dependent RNA polymerase. *PeerJ*, 8, e10480.
- Khaerunnisa, S., Kurniawan, H., Awaluddin, R., Suhartati, S., Soetjipto, S. 2020. Potential inhibitor of COVID-19 main protease (Mpro) from several medicinal plant compounds by molecular docking study. *Preprints*, 2020030226 (doi: 10.20944/preprints202003.0226.v1).
- Lee-Huang, S., Huang, P.L., Zhang, D., Lee, J.W., Bao, J., Sun, Y., Chang, Y.T., Zhang, J., Huang, P.L. 2007. Discovery of small-molecule HIV-1 fusion and integrase inhibitors oleuropein and hydroxytyrosol: Part I. fusion [corrected] inhibition. *Biochem. Biophys. Res. Commun.*, 354, 872-878.
- Li, H., Robertson, A.D., Jensen, J.H. 2005. Very fast empirical prediction and rationalization of protein pKa values. *Proteins*, 61, 704-721.
- Ma, S.C., He, Z.D., Deng, X.L., But, P.P., Ooi, V.E., Xu, H.X., Lee, S.H., Lee, S.F. 2001. In vitro evaluation of secoiridoid glucosides from the fruits of *Ligustrum lucidum* as antiviral agents. *Chem. Pharm. Bull.*, 49, 1471-1473.
- Malde, A.K., Zuo, L., Breeze, M., Stroet, M., Poger, D., Nair, P.C., Oostenbrink, C., Mark, A.E. 2011. An Automated Force Field Topology Builder (ATB) and Repository: Version 1.0. *J. Chem. Theory Comput.*, 7, 4026-4037.
- Monteil, V., Kwon, H., Prado, P., Hagelkrüys, A., Wimmer, R.A., Stahl, M., Leopoldi, A., Garreta, E., Del Pozo, C.H., Prosper, F. 2020. Inhibition of SARS-CoV-2 infections in engineered human tissues using clinical-grade soluble human ACE2. *Cell*, 181, 905-913. e907.
- Omar, S.H. 2010. Oleuropein in olive and its pharmacological effects. *Sci. Pharm.*, 78, 133-154.
- Pedretti, A., Villa, L., Vistoli, G. 2004. VEGA—an open platform to develop chemo-bioinformatics applications, using plug-in architecture and script programming. *Journal of computer-aided molecular design*, 18, 167-173.
- Pires, D.E., Blundell, T.L., Ascher, D.B. 2015. pkCSM: Predicting Small-Molecule Pharmacokinetic and Toxicity Properties Using Graph-Based Signatures. *J. Med. Chem.*, 58, 4066-4072.
- Raoult, D., Zumla, A., Locatelli, F., Ippolito, G., Kroemer, G. 2020. Coronavirus infections: Epidemiological, clinical and immunological features and hypotheses. *Cell Stress*, 4, 66.
- Sarikurku, C., Ozer, M.S., Istifli, E.S., Sahinler, S.S., Tepe, B. 2021. Chromatographic profile and antioxidant and enzyme inhibitory activity of *Sideritis leptoclada*: An endemic plant from Turkey. *South African Journal of Botany*, Doi: <https://doi.org/10.1016/j.sajb.2021.03.020>.
- Trott, O., Olson, A.J. 2010. AutoDock Vina: improving the speed and accuracy of docking with a new scoring function, efficient optimization, and multithreading. *J. Comput. Chem.*, 31, 455-461.
- Valdes-Tresanco, M.S., Valdes-Tresanco, M.E., Valiente, P.A., Moreno, E. 2020. AMDock: a versatile graphical tool for assisting molecular docking with Autodock Vina and Autodock4. *Biol. Direct*, 15, 12.
- Vicenti, I., Zazzi, M., Saladini, F. 2021. SARS-CoV-2 RNA-dependent RNA polymerase as a therapeutic target for COVID-19. *Expert Opin. Ther. Pat.*, 31, 325-337.
- Vijayan, R., Gourinath, S. 2021. Structure-based inhibitor screening of natural products

against NSP15 of SARS-CoV-2 revealed thymopentin and oleuropein as potent inhibitors. *J. Proteins Proteom.*, <https://doi.org/10.1007/s42485-021-00059-w>.

Wang, Y., Liu, M., Gao, J. 2020. Enhanced receptor binding of SARS-CoV-2 through networks of hydrogen-bonding and hydrophobic interactions. *Proc. Natl. Acad. Sci. USA*, 117, 13967-13974.